Implicit Discontinuous Galerkin Method for Hyperbolic Equations

Jorge L. D. Calle Philippe R B Devloo* Sônia M. Gomes†

Abstract

In this work a technique is presented for the numerical approximation of conservation laws. It is based both on the Runge-Kutta Discontinuous Galerkin method [3] and the Streamline Upwind Petrov-Galerkin method [2]. The proposed numerical scheme uses a discontinuous piecewise polynomial approximation in space and implicit backward Euler time stepping. Numerical oscillations within the discontinuous elements are controlled by adding a streamline diffusive term. An optimal relation between the time step (in terms of the CFL condition) and the size of the diffusion coefficient is anlysed for numerical precision. The scheme is implemented using the object oriented programming philosophy based on the enviroment described in [4]. Accuracy and shock capturing abilities of the method are analysed in terms of two bidimensional model problems, the rotating hill problem and the backward facing step problem for the Euler equations of gas dynamics.

Resumo

Neste trabalho, uma técnica para a aproximação numérica de leis de conservação é apresentada. Aproveitam-se idéias tanto do método Runge-Kutta Galerkin Descontínuo [3] quanto do método Streamline Upwind Petrov-Galerkin [2]. O esquema proposto usa aproxições polinomiais por partes descontínuas para a discretização espacial e o método de Euler implícito na discretização temporal. Para evitar oscilações numéricas, um termo difusivo é aplicado no interior dos elementos finitos, dispensando-se o uso de limitadores. Desenvolve-se um estudo para estabelecer uma relação adequada entre o valor do número CFL e o coeficiente máximo do termo difusivo, de tal forma a garantir a estabilidade do esquema e obter precisão numérica ótima. Implementa-se o esquema em um ambiente computacional usando a filosofia de programação orientada para objetos [4]. Para ilustrar a ordem de precisão e habilidade do método em capturar choques, apresentam-se resultados numéricos para dois problemas típicos bi-dimensionais, a rotação de um cone e o problema conhecido como backward facing step.

*FEC - UNICAMP, phil@fec.unicamp.br
†IMECC - UNICAMP, soniag@ime.unicamp.br

1 Introduction

The numerical solution of hyperbolic conservation laws is a topic of considerable importance for applications in several fields, particularly in fluid dynamics. Typically, solutions of conservation laws are characterized by spontaneous evolution of singular features which pose a considerable computational challenge. There is a great variety of modern alghorithms devised to achieve desired properties such as high-resolution, efficiency, stability, etc ([5],[6], [7]). In this paper, the discussion is concerned with two classes of methods that have been successfuly applied to conservation laws. Namely, the *Streamline Upwind Petrov-Galerkin (SUPG)* method [2] and the *Runge-Kutta Discontinuous Galerkin (RKDG)* method [3]. Both methods can be formulated in the same general framework that involves two basic steps.

- *Space discretization.* At each time step, an approximate solution is sought in a finite dimensional approximating space V_h. It is defined by imposing a Galerkin orthogonaly property (the residual is orthogonal to V_h). With proper choices of basis functions for V_h, the result is a system of ordinary differential equations.

- *Time discretization.* The resulting ODE system is discretized by an appropiate ODE solver.

In the SUPG method, the approximating spaces are, tipically, continuos finite elements and, for stability purposes, the original conservation law is perturbated by a term acting along characteristic directions. This perturbation can be thought of as a numerical diffusion term in the direction of the streamlines, whose magnitude is controlled in terms of a parameter δ, the so called artificial diffusion coefficient. Usually, increasing δ makes the scheme more stable (larger CFL numbers), but accuracy deteriorates. For the choice of δ, there must be a compromise between large CFL and accuracy. Increasing finite elements' order, basis functions get wider support, thus loosing efficiency.

In the RKDG method, the approximate solution is sought in a piecewise discontinuous polynomial space and an apropriate explicit Runge-Kutta method is applied in the time marching. To achieve stability, it also incorporates ideas of approximate Riemann solvers and slope limiters. High order schemes are possible with high degree of locality. However, slope limiters seem not to be a natural way of stabilization, since the procedure does not incorporate any intrisic property of the conservation law, neither suggests an easy implementation in higher dimensions.

Having these considerations in mind, it seems that the best qualities of both methods could be combined into a scheme that, instead of slope limiters, introduces local streamline diffusion terms to stabilize the discontinuous Galerkin method. This paper colects some illustrating results of our experiments in this direction.

In the very beginning, for simple 1D model problems, we realise that a diffusive term is unable to stabilize the explicit RKDG method without severe deterioration in accuracy. However, giving up the explicit approach, even with the simpliest first order Euler scheme,

the discontinuous Galerkin method with implicit streamline local diffusion terms shows good stability regions, regardless the polynomial interpolation order.

With an implicit method, a system of linear equations has to be solved at each time step. However, the corresponding matrices have simple block diagonal structures. This fact, combined with object oriented programming philosophy, which is based on the enviroment described in [4], led to efficient solvers.

The paper is organized as follows. In Section 2, there is brief overview of SUPG and RKDG methods. Section 3 is dedicated to the definiton of the new scheme, namely the discontinuous Galerkin method with implicit diffusive term (IDDG) and the study of its stability. In Section 4, accuracy and shock capturing abilities of the IDDG method are analysed in terms or two bidimensional model problems, the rotating hill problem and the backward facing step problem for the Euler equations.

2 SUPG and RKDG methods

In this section we present a brief review of the reference methods, SUPG and RKGM, aimed at solving systems of hyperbolic conservation laws in divergence form

$$\frac{\partial}{\partial t}u + \nabla.\mathbf{f}(u) = 0, \quad \mathbf{x} \in \Omega \subset R^d, \quad t > 0. \tag{1}$$

Here $\mathbf{f}(u) = (f_1(u), \cdots, f_d(u))$ is the d-dimensional flux and $u(t, \mathbf{x}) = (u_1(t, \mathbf{x}), \cdots, u_m(t, \mathbf{x}))$ is the unknown m-vector, subjected to initial condition

$$u(0, \mathbf{x}) = u_0(\mathbf{x}). \tag{2}$$

Eventually, apropriate boundary conditions are also imposed.

Let us suppose that Ω has been subdivided into a finite element partition M_h. On this partition, we consider finite element spaces V_h consisting of piecewise polynomial of fixed degree $p \geq 0$. This means that, if $w \in V_h$, then $w|_C \in \Pi_p$. Let

$$B_{V_h} = \{\varphi_i(\mathbf{x}), \quad i = 1, 2, \ldots, N\}$$

denotes a set of linearly independent basis spanning V_h. The approximate solution is sought in the form

$$u_h(t, \mathbf{x}) = \sum_{j=1}^{N} u_i(t)\varphi_i(\mathbf{x}).$$

In a standard Galerkin formulation, we seek u_h such that for all $j = 1, 2, \cdots, N$,

$$\frac{\partial}{\partial t}\int_\Omega \varphi_j u_h - \int_\Omega \nabla\varphi_j.\mathbf{f}(u_h) + \int_{\partial\Omega} \varphi_j \mathbf{f}(u_h).\tilde{\eta} = 0, \tag{3}$$

where $\tilde{\eta}$ denotes the unit outward normal vector to Ω. However, this kind of formulation ends up being highly unstable.

⋆ **The SUPG method**

The SUPG method is characterized by the replacement of equation (3) by the perturbed one

$$\frac{\partial}{\partial t}\int_\Omega \varphi_j u_h - \int_\Omega \nabla\varphi_j.\mathbf{f}(u_h) + \int_{\partial\Omega} \varphi_j \mathbf{f}(u_h).\tilde{\eta} - \delta\int_\Omega (\nabla\varphi_j.\beta)\,\nabla.\mathbf{f}(u_h) = 0. \tag{4}$$

The additional term

$$\delta\int_\Omega (\nabla\varphi_j.\beta)\,\nabla.\mathbf{f}(u_h),$$

where β is a vector of matrices, is usually called diffusive term. In the unidimensional case, the expression $\nabla\varphi_i.\beta$ is interpreted as

$$\nabla\varphi_i.\beta = \frac{d\varphi_i}{dx}\beta,$$

whereas, in the bidimensional case, $\beta = (\beta_1, \beta_2)$ and

$$\nabla\varphi_i.\beta = \frac{\partial\varphi_i}{\partial x}\beta_1 + \frac{\partial\varphi_i}{\partial y}\beta_2.$$

In the literature, there are several ways of defining β. In the present work, the expression of β is given as in [1]

- **Unidimensional case**

$$\beta = \frac{\Delta x}{2} f_1^{'}|f_1^{'}|.$$

- **Bidimensional case**

$$\beta = (f_1^{'}\tau, f_2^{'}\tau),$$

where

$$\tau = \left[\left|\frac{\partial\xi}{\partial x}f_1^{'} + \frac{\partial\xi}{\partial y}f_2^{'}\right| + \left|\frac{\partial\eta}{\partial x}f_1^{'} + \frac{\partial\eta}{\partial y}f_2^{'}\right|\right]^{-1}.$$

⋆ **The RKDG method**

In the RKDG method, the functions in V_h are discontinuous and each of the basis functions $\varphi_i \in B_{V_h}$ is supported in a single cell of the partition M_h. Therefore, in the Galerkin formulation (3), the integrals may be restricted to the cells of the partition. Because of discontinuities on the cell boundaries, the flux must be replaced by a *approximate Riemann solver* or *numerical flux* $\hat{\mathbf{f}}(u_h)$. Therefore, the numerical solution $u_h \in V_h$ is found such that

$$\frac{\partial}{\partial t}\int_C \varphi_j u_h - \int_C \nabla\varphi_j.\mathbf{f}(u_h) + \int_{\partial C} \varphi_j \hat{\mathbf{f}}(u_h).\eta_C = 0, \tag{5}$$

for all $C \in M_h$ and $j = 1, \cdots, N$. The time discretization is performed by special explicit high-order accurate Runge-Kutta methods. If u_h^n is the solution at $t = t_n$, the the solution at the next time-step u_h^{n+1} is obtained after L intermediate steps, by the time-marching algorithm

1. $\tilde{u}_h^{(0)} = u_h^n$;
2. For $\ell = 1, \cdots, L$

$$\sum_{i=1}^{N} \tilde{u}_i^{(\ell)} \int_C \varphi_i \varphi_j = \int_C u_h^n \varphi_j + \Delta t_n \sum_{k=0}^{\ell-1} c_{\ell k} \left\{ \int_C \nabla \varphi_j . \mathbf{f}(\tilde{u}_h^k) - \int_{\partial C} \varphi_j \hat{\mathbf{f}}(\tilde{u}_h^k) . \eta_C \right\} \tag{6}$$

   where $\tilde{u}_h^k = \sum_{i=1}^{N} \tilde{u}_i^k \varphi_i$.

3. $u_h^{n+1} = \tilde{u}_h^{(L)}$.

At each intermediate step of this algorithm, there is a system to be solved

$$K \tilde{u}^\ell = F,$$

where K is the mass matrix with entries

$$K_{ij} = \int_C \varphi_i \varphi_j,$$

and right hand side

$$F_j = \int_C u_h^n \varphi_j + \Delta_k \sum_{k=0}^{\ell-1} c_{\ell k} \left\{ \int_C \nabla \varphi_j . \mathbf{f}(\tilde{u}_h^k) - \int_{\partial C} \varphi_j \hat{\mathbf{f}}(\tilde{u}_h^k) . \tilde{\eta}_C \right\}.$$

As noted in [3], the choice of the numerical flux does not have a significant impact on the quality of the approximations, regardless the polynomial interpolation degree. Therefore, in all experiments of the present paper, the simple Lax-Friederics numerical flux shall be used.

In the piecewise constant case ($p = 0$), and forward Euler scheme in time, the scheme corresponds to the usual finite volume method. Typically, if the numerial flux is choosen so that the scheme is monotone, and the problem is for a scalar conservation law, them it is possible to prove the stability and convergence of the method [6]. For higher order polynomials $p \geq 1$, and Runge-Kutta of order $p + 1$, and Lax-Friederics numerical flux, it is suggested in [3] that, for stability, the relation

$$|\max f^{'}(u)| \frac{\Delta t}{\Delta x} \leq CFL \tag{7}$$

must be considered with

$$CFL = \frac{1}{2p+1}. \tag{8}$$

In practical applications, with sharp gradient variations, the CFL condition (8) implies very small time steps and efficiency is lost. Usually, to overcome this difficulty, *slope limiters* are enforced, at each intermediate step, by means of a non-linear projection operator. It is possible to construct slope limiters that ensure stability, without degrading the accuracy [3]. The use of a slope limiter is crucial, mainly when shocks are present. Its action is similar to the introduction of diffusion in the interior of the elements, in order to avoid internal oscillations. The slope limiter forces the solution to be under control, according to the values on the neighboring elements. Its definition does not depend on the conservation law at hand.

3 Diffusive discontinuous Galerkin method

Our purpose is to use artificial diffusion, instead of slope limiters, in order to stabilise the Discontinuous Galerkin Method. Therefore, we combine formulations (3) and (5) by considering the new formulation of finding a discontinuous piecewise polynomial solution $u_h \in V_h$ such that for all $C \in M_h$

$$\frac{\partial}{\partial t}\int_C \varphi_j u_h - \int_C \nabla\varphi_j.\mathbf{f}(u_h) + \int_{\partial C} \varphi_j \hat{\mathbf{f}}(u_h).\eta_C - \delta \int_C (\nabla\varphi_j.\beta)\,\nabla.\mathbf{f}(u_h) = 0, \tag{9}$$

where β is determined as in the SUPG method. Therefore, the intermediate steps in the Runge-Kutta algorithm reads

$$\begin{aligned}\sum_{i=1}^{N} \tilde{u}_i^{(\ell)} \int_C \varphi_i\varphi_j = \int_C u_h^n\varphi_j + \Delta t_n \sum_{k=0}^{\ell-1} c_{\ell k} \Big\{ \int_C \nabla\varphi_j.\mathbf{f}(\tilde{u}_h^k) \\ - \int_{\partial C} \varphi_j \hat{\mathbf{f}}(\tilde{u}_h^k).\eta_C + \delta \int_C (\nabla\varphi_j.\beta) \sum_{s=1}^{d} f_s'(\tilde{u}_h^k)\frac{\partial}{\partial x_s}\tilde{u}_h^k \Big\}.\end{aligned} \tag{10}$$

As a test model problem, consider the scalar linear conservation law, with $\mathbf{f}(u) = u$, defined on the unit interval $\Omega = [0,1]$, with periodic boundary conditions and initial data

$$u_0(x) = \begin{cases} 1, & 0 \le x \le 0.5 \\ 0, & 0.5 \le x \le 1. \end{cases}$$

The scheme (10) is applied for different CFL and δ parameters within the following range

- $0.1 \le CFL \le 1$, with increment 0.1.
- $0 \le \delta \le 1$, with increment 0.05.

The next results are for a partition of 50 finite elements, and Runge-Kutta of order $p+1$ for polynomial interpolation of degree p. The errors are measured in the $||.||_{L^1}$ norm. The

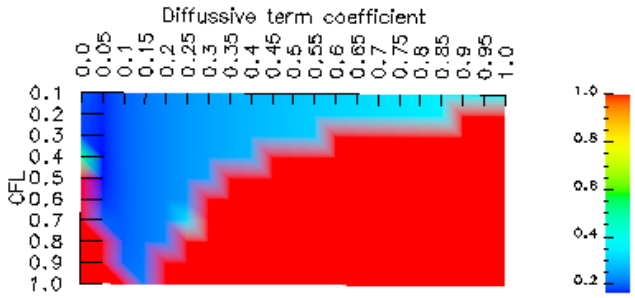

p=1 : Errors to continuous and Runge–Kutta(2) scheme

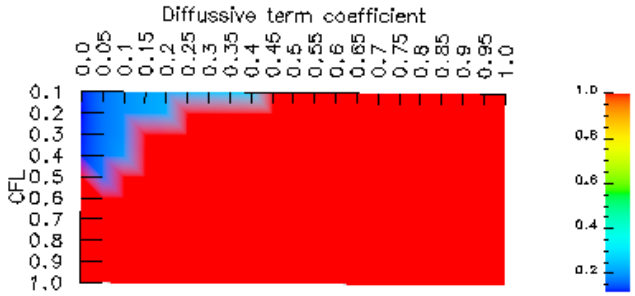

p=2 : Errors to continuous and Runge–Kutta(3) scheme

Figure 1: Stability region: explicit diffusion and continuous basis functions.

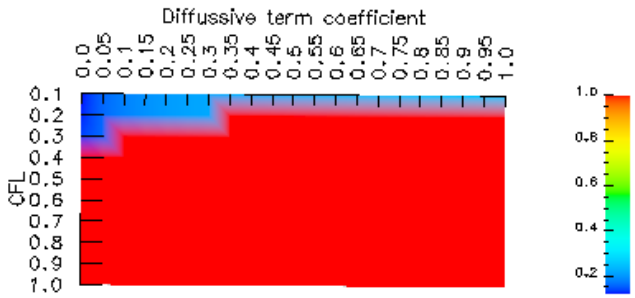

p=1 : Errors to discontinuous and Runge−Kutta(2) scheme

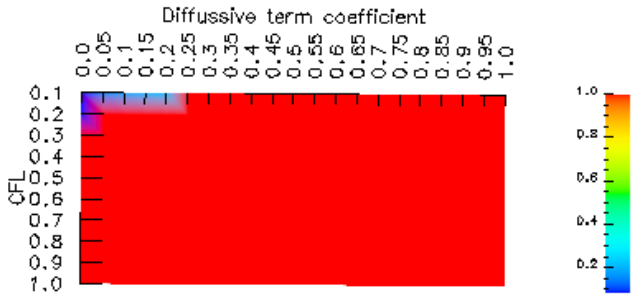

p=2 : Errors to discontinuous and Runge−Kutta(3) scheme

Figure 2: Stability region: explicit diffusion and discontinuous basis functions .

red colour corresponds to unstable regions. For the sake of comparison, similar experiments are carried out for the SUPG method, with continuous approximating functions of the same degree. Figure 1 corresponds to the results for SUPG with continuous piecewise polynomials of degree $p = 1$ and $p = 2$. The equivalent results for the discontinuous Galerkin method with diffusive term are presented in Figure 2. Based on these results, the following concluding remarks are in order:

1. Without viscosity term $\delta = 0$, the Runge-Kutta Galerkin method is stable for $CFL \leq \frac{1}{2p+1}$, for both continuous and discontinuous approximating spaces;

2. The experiments with discontinuous approximating functions show smaller error amplitudes than with continuous ones;

3. In both cases, the smallest errors occur when the Runge-Kutta Galerkin scheme is

applied without the diffusion term. The errors increase with increasing diffusive coefficient;

4. The addition of the diffusive term is not sufficient to make the scheme stable if the CFL number is mantained greater than $\frac{1}{2p+1}$.

3.1 IDDG method

Moved by the negative results just described, the next step would be to consider a scheme where the diffusive term is treated implicitly. However, the implementation of an implicit Runge-Kutta scheme would require the computation of the stiffness matrix at each intermediate step. Having this difficulty in mind, a single step backward Euler scheme is tried first. In this case, formula (10) reduces to

$$\sum_{i=1}^{N} u_i^{n+1} \int_C \left[\varphi_i \varphi_j + \delta \Delta t_n \left(\nabla \varphi_j . \beta \right) \sum_{s=1}^{d} f_s^{'}(u_h^{n+1}) \frac{\partial}{\partial x_s} \varphi_i \right] = \int_C u_h^n \varphi_j + \Delta t_n \left\{ \int_C \nabla \varphi_j . \mathbf{f}(u_h^n) - \int_{\partial C} \varphi_j \hat{\mathbf{f}}(u_h^n) . \eta_C \right\}. \quad (11)$$

We have special interest in discontinuous finite elements approximating spaces. However, the continuous case is also considered, for comparsion purposes.

3.1.1 Stability analysis: linear case

The model problem is the same one considered before. The black dot lines in Figures 3 and 4 correspond to the occurrence of the smallest errors, indicating the optimal compromise between the parameters CFL and δ for the corresponding scheme.

In Figure 3, the results for the case of continuous approximating functions with degree $p = 1, 2$ and 3 are displayed. Since this is a close variation of the classical SUPG method, their performance are also similar.

⋆ **SUPG with implicit diffusion**

- The scheme is stable when the diffusion coefficient δ and the CFL parameter satisfy the relation $\delta \geq 0.5 CFL$;
- The smallest errors occur when $\delta \sim 0.5 CFL$. This means that the best approximation occurs when the scheme becomes stable, and increasing the diffusive term deteriorates the accuracy.

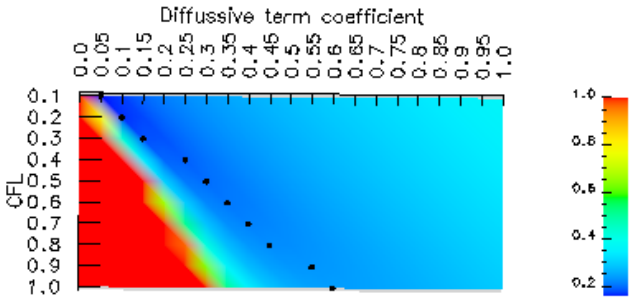

p=1 : Errors to continuous and implicit scheme

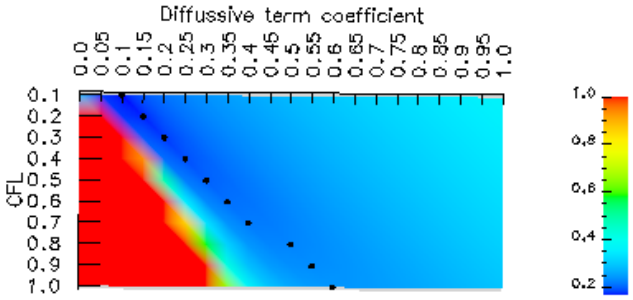

p=2 : Errors to continuous and implicit scheme

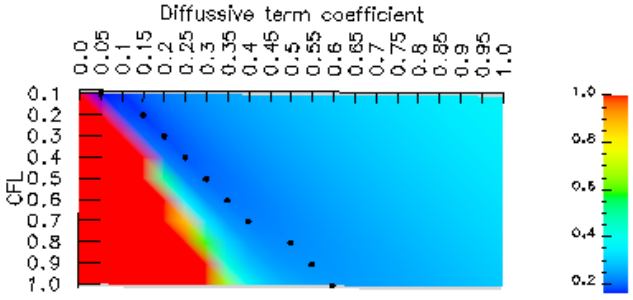

p=3 : Errors to continuous and implicit scheme

Figure 3: Stability region: implicit diffusion and continuous basis funcions

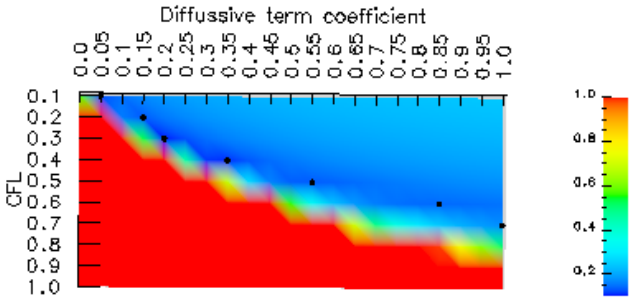

p=1 : Errors to discontinuous and implicit scheme

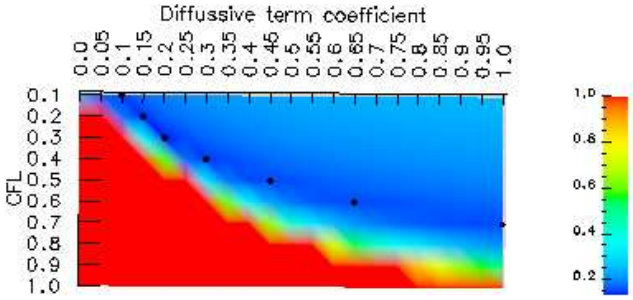

p=2 : Errors to discontinuous and implicit scheme

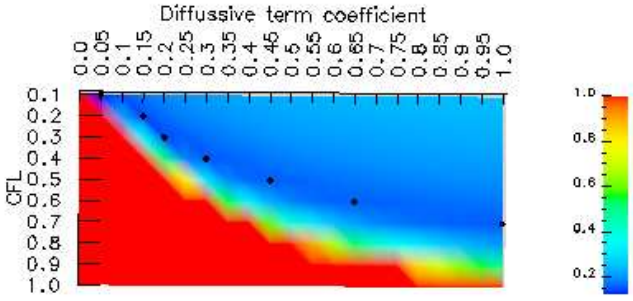

p=3 : Errors to discontinuous and implicit scheme

Figure 4: Stability region: implicit diffusion and discontinuous basis functions

Figure 4 corresponds to the case of discontinuous approximating functions with degree $p = 1, 2$ and 3. The following aspects are highlighted.

⋆ **IDDG method**

- The stability region occurs when the diffusive coefficient δ and the CFL parameter satisfy the relation
$$\delta \geq \frac{10}{3}CFL^2 - \frac{2}{3}CFL + \frac{1}{10};$$
- The smallest errors also occur close to the boundary of the stability region
$$\delta \sim \frac{10}{3}CFL^2 - \frac{2}{3}CFL + \frac{1}{10}.$$
This means that the best approximation and stability occur simultaneously, and increasing the diffusive term deteriorates the accuracy. The best performance is for $\delta = 0.2$ and $CFL = 0.3$.
- When compared with the results of Figure 3, the errors with discontinuous approximating functions are smaller than with continuous ones;
- The deterioration of the accuracy with increasing diffusion coefficient is less pronouced in the case of discontinuous approximating functions. When using continuous approximating functions, the strong diffusive term smoothens the solution too much close to discontinuites.
- Increasing the diffusive term in the IDDG method, the numerical solution tends to become constant into the cells. In this sense, with high diffusive terms, the IDDG method behaves like the classical finite volume scheme.

3.1.2 Stability analysis: nonlinear case

Consider the unidimensional Burgers equation, with periodic boundary conditions on the interval $[-1, 2]$, and initial condition

$$u_0(x) = \begin{cases} 1 & -1 \leq x \leq 0.25 \\ 0 & 0.25 \leq x \leq 0.75 \\ -1 & 0.75 \leq x < 2. \end{cases}$$

The implicit scheme (11) is applied with continuous and discontinuous approximanting functions of degree $p = 1$, in a grid of 50 finite elements. Figures 5 and 6 display the error magnitude in both experiments. The following conclusions hold:

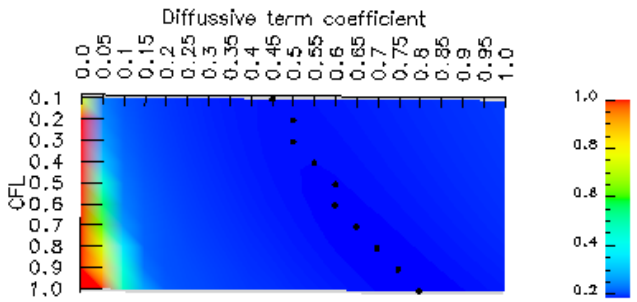

Figure 5: Stability region: implicit difusion and continuous basis functions.

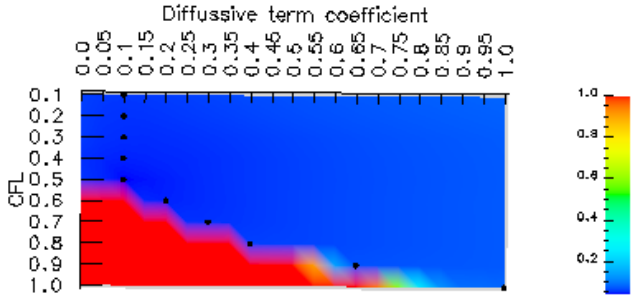

Figure 6: Stability region: implicit diffusion and discontinuous basis functions.

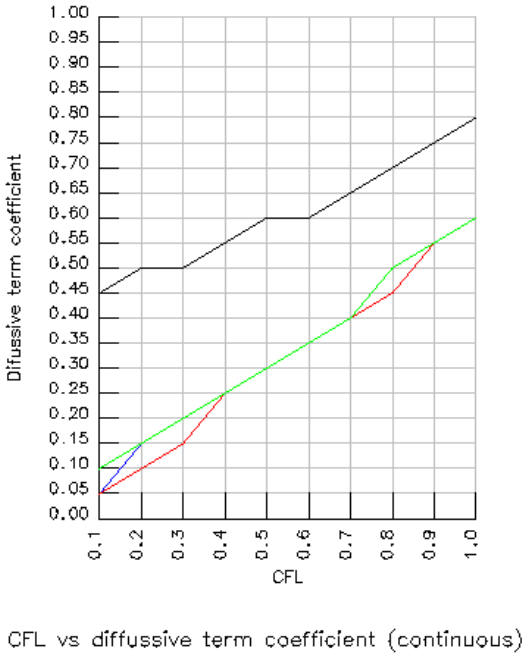

Figure 7: Optimal relation between CFL and δ for continuous basis functions.

- As in the linear problem, when continuous approximating functions are used, there is a linear best compromise between δ and CFL. However, for the Burgers equation, the optimal curve is in the interior of the stability region;
- When using discontinuous approximating functions, δ and CFL are quadraticaly related to get the best performance and the optimal curve is close to the boundary of the stability region;
- The stability region for continuous approximating functions is wider than for discontinuous ones. However, inside the stability region, the accuracy is better for discontinuous approximating functions than for continuous ones.

3.1.3 Optimal relation between δ and CFL

In Figures 7 and 8, the curves relating the diffusive coefficient δ and the CFL parameter that give the best accuracy in the experiments described above, are plotted. As shown in the botton part of Figure 7, when using continuous approximating functions to solve the linear problem, the curves corresponding to $p = 1, 2$ and 3 almost coincide. The best linear

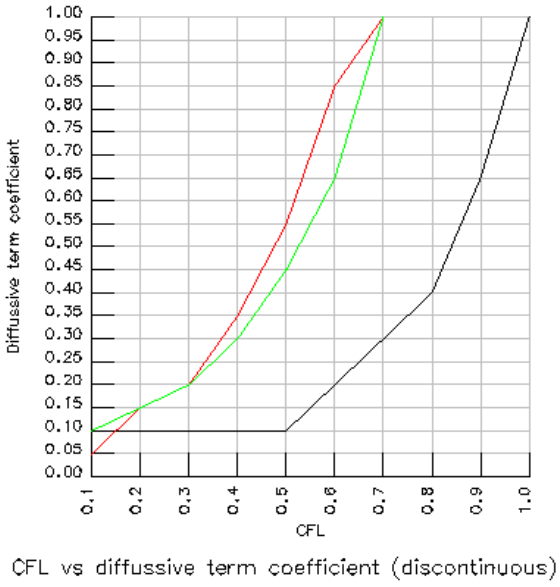

Figure 8: Optimal relation between CFL and δ for discontinuous basis functions.

correlation gives

$$\delta = \frac{1}{2}CFL + \frac{1}{20}.$$

The curve in the upper part corresponds to the Burgers equation and it shows the linear correlation

$$\delta = \frac{1}{2}CFL + \frac{3}{10}.$$

In the case of discontinuous approximating functions and linear problem, the correlation seems to be quadratic, and it is also independent of the interpolation degree, as shown in the upper part of Figure 8. The correlation is

$$\delta = \frac{10}{3}CFL^2 - \frac{2}{3}CFL + \frac{1}{10}.$$

The curve corresponding to the nonlinear Burgers equation is shown in the lower part of the same figure and the correlation seems also to be quadratic. However, since the optimal curve is very close to the limit of the stability region, such relations seem not to be useful.

4 Accuracy and shock capturing tests

The stability results, presented in the previous sections for 1D model problems, are indicators of the good performance properties of the proposed IDDG scheme. In this section, some typical expamples in 2D are considered that confirm this expectation. For accuracy analysis, we shall consider the rotating hill problem. To analyse the ability of capturing strong shocks, we shall consider the backward-facing step problem for the Euler equations.

4.1 The rotating hill problem

For $\Omega = [-5,5]\times[-5,5] \subset R^2$, $\mathbf{x} = (x,y) \in \Omega$, and $u \in R$, we consider the linear conservation law with flux given by $f_1(u) = -yu$ and $f_2(u) = xu$, initial condition

$$u_0(\mathbf{x}) = \begin{cases} 2.5(1+\cos(\frac{2\pi}{3}||\mathbf{x}-\mathbf{x}_0||) & ||\mathbf{x}-\mathbf{x}_0|| \le 1.5 \\ 0 & ||\mathbf{x}-\mathbf{x}_0|| < 1.5 \end{cases},$$

where $\mathbf{x}_0 = (0, 2.5)$, and boundary conditions $u(t,\mathbf{x}) = 0, \mathbf{x} \in \Omega$. The exact solution is such that at $t = 2\pi$ it is back to its initial position, after a complete rotation around the origin.

For accuracy analysis, we consider a sequence of triangular grids which are obtained by diagonal cell subdivision of regular retangular grids, with $\Delta_x = \Delta_y$, but the parameters $CFL = 0.6$ and $\delta = 0.1$ are kept constant in all the cases. The level sets of the numerical solution obtained with $p = 1$ and $\Delta_x = 0.2$ are shown in Figure 9, at $t = 0, t = \pi, t = 7\pi/5$ and $t = 2\pi$. Varying Δ_x, the L_1 error measures are shown in Figure 10.

4.2 Backward facing step

The next example considers the Euler equations on the L-shaped region

$$\Omega = [0.,0.6] \times [0.,0.2] \cup [0,3.] \times [0.2,1.],$$

as displayed in Figure 11. For the boundary conditions we consider: on the left, Dirichlet boundary condition $u = u_0$, where u_0 is the initial condition; wall boundary condition on the botton $\partial\Omega_2$ and on the top $\partial\Omega_3$; and free flow on the right $\partial\Omega_4$. Interpolation of degree $p = 1$, $CFL = 0.4$ and $\delta = 0.75$. Level sets for the numerical density calculations are shown in Figure 12 at $t = 0.1$, $t = 0.58$, $t = 1.$ and $t = 2.$, showing the formation and evolution of the shock around the corner. The preassure level set at $t = 0.78$, and close to the steady state $t = 1.8$ are shown in Figure 13.

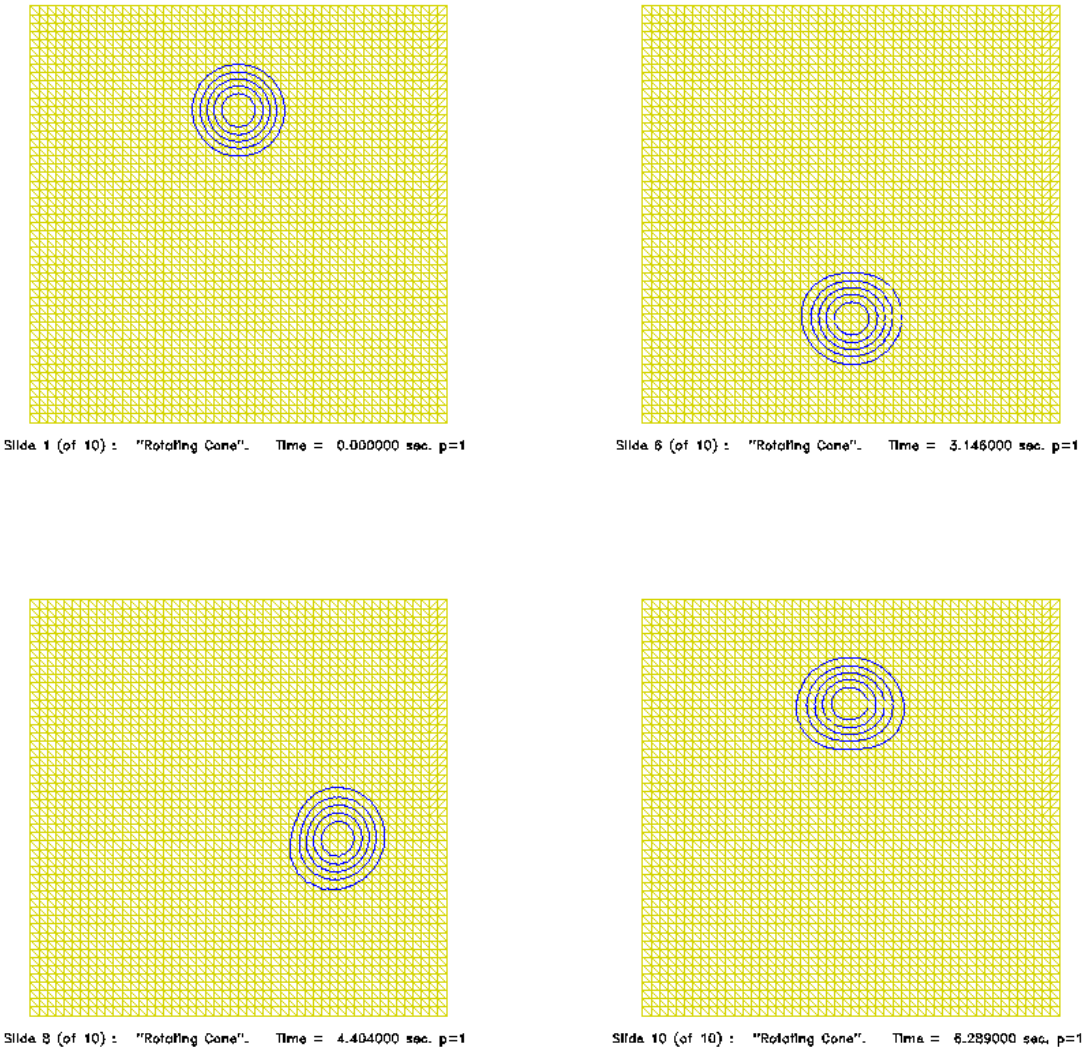

Figure 9: Rotating hill: mesh and level sets at $t = 0$, $t = \pi$, $t = 7\pi/5$ e $t = 2\pi$.

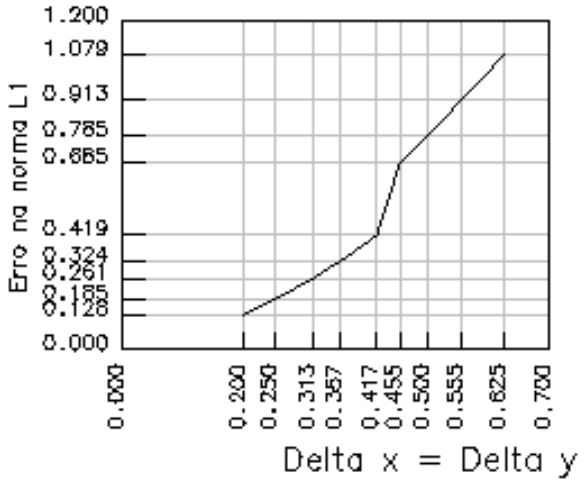

Figure 10: Convergence analysis: L_1 errors.

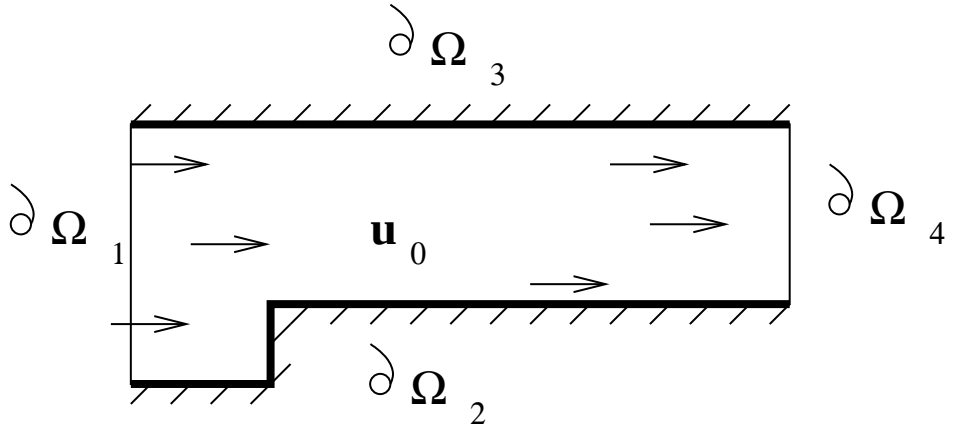

Figure 11: Computational domain.

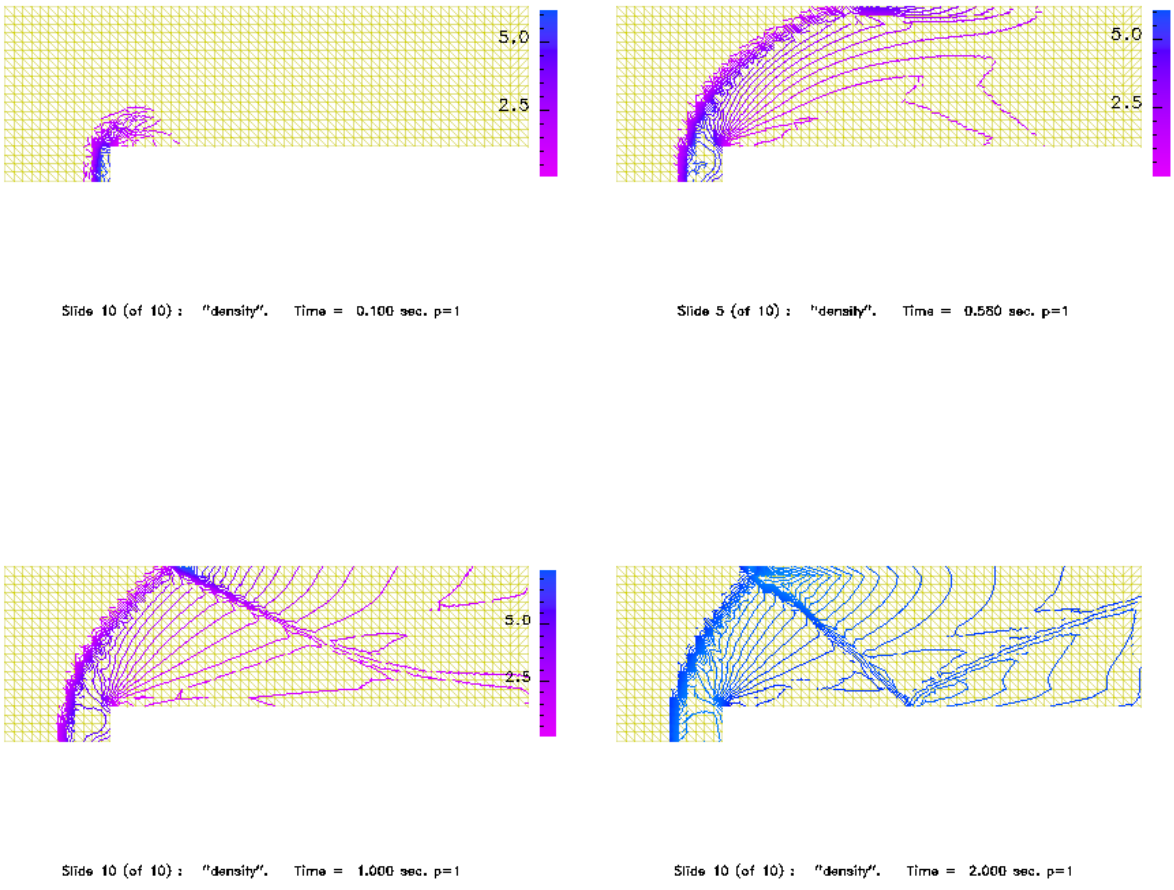

Figure 12: Density level sets at $t = 0.1$, $t = 0.58$, $t = 1.$ and $t = 2.$

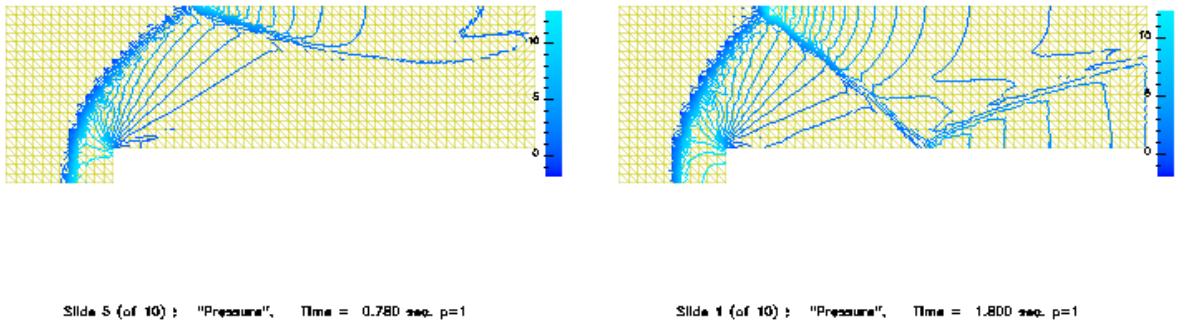

Figure 13: Pressure level sets at $t = 0.78$ and $t = 1.8$.

References

[1] Daryl Lawrence Bonhaus. *A higher order accurate finite element method for viscous compressible flows.* PhD thesis, Virginia Polytechnics Institute and State University, November 1998.

[2] A. Brooks and T. Hughes. Streamline upwind/petrov-galerkin formulations for convection dominated flows with particular emphasis on the incompressible navier-stokes equations. *Comp. Meth. Applied Mechanics*, Engng. 32, 1982.

[3] Bernardo Cockburn and Chi-Wang Shu. Runge-kutta discontinuous galerkin method for convection-dominated problems. Journal of Scientific Computing, 2001.

[4] Philippe Remy Bernard Devloo. Pz: An object oriented environment for scientific programming. *Computer Methods in Applied Mechanics and Engineering*, 150, 1997. Dedicated to J.T. Oden.

[5] Edwige Godlewski and Pierre-Arnaud Raviart. *Hyperbolic Systems of Conservation Laws.* Mathématiques & Applications. Ellipses., France, 1991.

[6] Dietmar Kroner. *Numerical schemes for conservation laws.* Wiley-Teubner series, advances in numerical mathematics, 1997.

[7] J. Randall and Le Veque. *Numerical Methods for Conservation Laws.* Birkhäuser Verlag, Berlin, 1990.